RSC Advances

Cite this: *RSC Advances*, 2012, **2**, 12263–12268

www.rsc.org/advances

PAPER

Mesoporous silica-coated $NaYF_4$ nanocrystals: facile synthesis, *in vitro* bioimaging and photodynamic therapy of cancer cells

Xinhui Liu,[a] Haisheng Qian,*[ab] Yaping Ji,[a] Zhengquan Li,[a] Yong Shao,[ab] Yong Hu,[ab] GuoXiu Tong,[ab] Liangchao Li,[ab] Weidong Guo*[a] and Huichen Guo*[c]

Received 3rd August 2012, Accepted 7th October 2012
DOI: 10.1039/c2ra21688d

Up-conversion nanoparticles (UCNPs) that emit high-energy photons upon excitation by low-energy near-infrared (NIR) radiation are emerging as new optical nanoprobes useful in biomedicine. Herein, the one pot facile synthesis of mesoporous silica-coated $NaYF_4$:Yb/Er nanoparticles has been achieved successfully. The as-prepared product was characterized by X-ray power diffraction (XRD), transmission electron microscopy (TEM) and Brunauer–Emmet–Teller (BET) surface area analyses, respectively. The resulting nanoparticles with a BET area of 800 $m^2\ g^{-1}$ and an average pore size of 2.6 nm were spherical, highly monodispersed and stable in an aqueous system. Furthermore, the $NaYF_4$:Yb/Er@mesoporous silica nanoparticles also displayed good biocompatibility and could be used for bio-labeling or bio-imaging. Additionally, the results of preliminary photodynamic therapy (PDT) of cancer cells indicated the $NaYF_4$:Yb/Er@mesoporous silica nanoparticles could be used as important photosensitizer carriers for tumor therapy.

Introduction

Photodynamic therapy (PDT) is considered to be both minimally invasive and toxic; these advantages alone make PDT an attractive alternative to traditional cancer treatments.[1–3] Up-conversion nanoparticles (UCNPs) have received much attention due to their potential applications in fluorescent imaging probes, photodynamic therapy (PDT) of cancer cells *etc.*[4–10] It is well known that Yb/Er (or Yb/Tm) co-doped hexagonal-phase $NaYF_4$ nanocrystals are the most efficient NIR-to-visible up-conversion material due to their low phonon energy loss from the $NaYF_4$ crystal lattice.[11] In recent years, much effort has been paid to synthesize rare earth ionic-doped $NaYF_4$ nanocrystals. A variety of techniques have been successfully employed to synthesize Yb/Er (or Yb/Tm) co-doped hexagonal-phase $NaYF_4$ nanocrystals with different sizes and shapes.[12–18]

The protocol for the PDT of cancer cells using UCNPs as remote controlled nano-transducers was illustrated as follows: UCNPs are endowed with an up-converting property and can convert near-infrared (NIR) light to different wavelengths of visible light upon excitation by just a single 980 nm wavelength. Spectral overlap between the emitted light which peaks at both the green and red regions and the maximum absorption wavelengths of the respective loaded photosensitizers in mesoporous silica layers, activate these drugs to generate cytotoxic $^1O_2$ and further kill cancer cells. According to our previous study, the most important requirement for the PDT of cancer cells involved the synthesis of mesoporous silica-coated UCNPs with a higher specific surface area. However, the hexagonal $NaYF_4$ nanocrystals obtained from the majority of the above methods are highly hydrophobic and cannot be dispersed into water or ethanol. Thus, it is important to convert hydrophobic UCNPs into water-soluble UCNPs by directly oxidizing oleic acid ligands with Lemieux-von Rudloff reagent[19] or by the microemulsion process employed to synthesize $NaYF_4$/silica core/shell nanoparticles.[20] Furthermore, the fluorescence signal from the mesoporous silica-coated $NaYF_4$ nanoparticles can be strengthened by increasing the input power of the NIR laser; alternatively, a few $NaYF_4$ nanocrystals can be aggregated together and encapsulated into one single silica shell to enhance the total fluorescence intensity. In addition, as a result of the specific surface area being obviously increased after the formation of a coated mesoporous structure shell, many more photosensitizers could be adsorbed onto the surface of the mesoporous silica, releasing more reactive singlet oxygen to kill cancer cells.

Herein, a facile one-pot chemical approach has been developed to synthesize mesoporous silica-coated $NaYF_4$ nanocrystals by an improved microemulsion method. The as-prepared $NaYF_4$:Yb/Er@mesoporous silica nanoparticles have an ideal surface area and displayed good biocompatibility. The PDT

[a]*Department of Chemistry, College of Chemistry and Life Sciences, Zhejiang Normal university, Jinhua, 321004, P. R. China. E-mail: gwd@zjnu.cn*
[b]*Institute of Physical Chemistry, Zhejiang Normal University, Jinhua, 321004, P. R. China. E-mail: shqian@zjnu.cn; Fax: +86-579-82282269; Tel: +86-579-82282269*
[c]*State Key Laboratory of Veterinary Etiological Biology and Key Laboratory of Animal Virology of Ministry of Agriculture, Lanzhou Veterinary Research Institute, Chinese Academy of Agricultural Sciences, Xujiaping 1, Lanzhou, Gansu, 730046, P. R. China. E-mail: ghch-2004@hotmail.com*

effect *in vitro* confirmed that $NaYF_4$:Yb/Er@mesoporous silica nanoparticles could be useful carriers for photosensitizers—labels of bio-imaging.[21–22]

Results and discussion

The first step of the process is to achieve the hexagonal phase $NaYF_4$:Yb/Er nanocrystals with uniform size distribution *via* an efficient and user-friendly method.[23–24] Fig. 1 shows the typical transmission electron microscopy (TEM) images of the $NaYF_4$:Yb/Er nanocrystals. The general overview of the TEM images (Fig. 1a and b) indicated that the products were uniform sphere-like nanocrystals with an average diameter of 20 nm. Fig. 1c presented the typical XRD pattern of the as-prepared samples. All the peaks could be indexed to the hexagonal-phase $NaYF_4$ crystals with cell parameters of a = 5.96 Å and c = 3.51 Å (JCPDS Data File no. 28-1192). No impurity peaks were observed, indicating the high purity of the final products.

Morphology characterization of silica or mesoporous silica-coated $NaYF_4$ nanoparticles

Octadecyltrimethoxysilane (C18TMS) is an organosilicon compound, which has been used for preparing hydrophobic coatings and self-assembled monolayers[25] such as mesoporous silica coatings on $NaYF_4$/silica,[26] SiO_2/Fe_2O_3[27] and Au@silica.[28] The suitable amount of octadecyltrimethoxysilane and the concentration of $NaYF_4$:Yb/Er nanocrystals played a key role in producing silica-coated $NaYF_4$:Yb/Er nanoparticles with different sizes and shapes, as well as the homogeneity of particle. Fig. 2 shows the TEM images of the $NaYF_4$:Yb/Er@silica core/shell nanoparticles with different $NaYF_4$:Yb/Er loading. Fig. 2a shows that a thin and uniform silica shell was coated on the single nanoparticle and the thickness of the silica shell was about

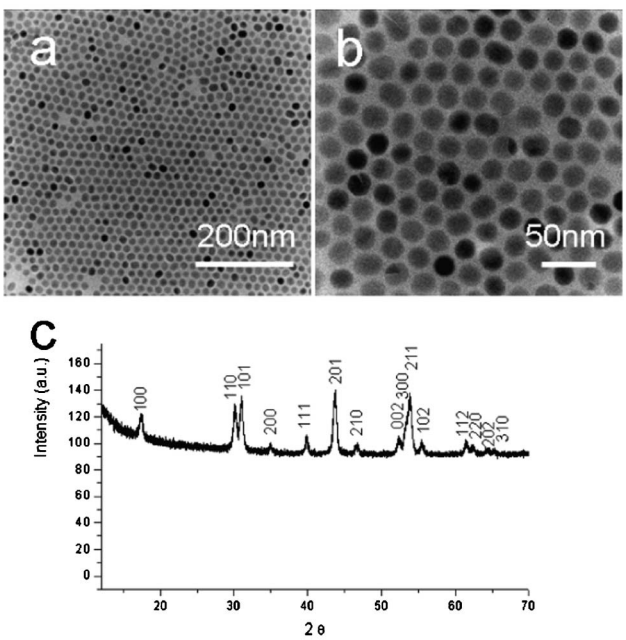

Fig. 1 TEM images of the $NaYF_4$:Yb/Er nanocrystals: (a) low magnification; (b) high magnification. (c) XRD patterns of the as-prepared Yb/Er-codoped $NaYF_4$ nanocrystals.

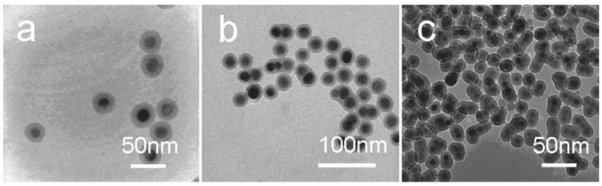

Fig. 2 TEM images of silica-coated nanocrystals with different nanostructures obtained from 200 uL TEOS and 40 mL $NaYF_4$ nanocrystal/cyclohexane solution with different concentrations in the absence of octadecyltrimethoxysilane (C18TMS) and with other conditions kept constant. (a) 0.01 M; (b)0.02 M; (c) 0.04 M.

10 nm when the concentration of the nanocrystals was 0.01 M. When the concentration of the nanocrystals was increased to 0.04 M, it was found that there were 2–3 $NaYF_4$ nanoparticles incorporated into a single silica shell (Fig. 2c). The thickness of the silica shell was *ca.* 10 nm. The total size of $NaYF_4$:Yb/Er@silica was still smaller than 50 nm, which is an appropriate size for biological studies and clinical applications.

Fig. 3 shows TEM images of silica-coated $NaYF_4$:Yb/Er nanoparticles obtained from 200 μL TEOS, 80 μL octadecyltrimethoxysilane (C18TMS) and a cyclohexane solution of $NaYF_4$:Yb/Er nanocrystals (40 mL, 0.04 M) before and after calcination at 500 °C for 2 h. As shown in Fig. 3a, the TEM image clearly demonstrated the $NaYF_4$:Yb/Er@silica core–shell structure, with every core–shell nanoparticle composed of 2–3 $NaYF_4$ nanoparticles and a thin amorphous silica shell with a thickness of 20 nm. From the TEM images shown in Fig. 3b and c, the porous structure of the silica shell could be observed clearly, which has a similar thickness of 20 nm. The up-conversion fluorescent properties of the mesoporous silica coated on $NaYF_4$:Yb/Er nanoparticles was characterized and is shown in Fig. 3d, the emission peaks located at 408, 522, 542 and 655 nm were attributed to the transitions from $^4H_{9/2}$, $^4H_{11/2}$, $^4S_{3/2}$ and $^4F_{9/2}$ to $^4I_{15/2}$ of Er^{3+}, respectively. This is in good agreement with the as-prepared nanocrystals.[23,29]

BET analysis

Fig. 4 shows the N_2 adsorption–desorption isotherms and pore-size distribution curves of the as-prepared mesoporous silica-coated $NaYF_4$:Yb/Er nanoparticles (shown in Fig. 3b and c), in which the N_2 adsorption–desorption isotherms could be classified as type IV isotherms according to the International Union of Pure and Applied Chemistry (IUPAC) nomenclature.[30] The mesoporous silica-coated $NaYF_4$:Yb/Er nanoparticles have a Brunauer–Emmett–Teller surface area of 800 $m^2\ g^{-1}$ (Fig. 4a) and an average pore size of *ca* 2.6 nm, suggesting a mesoporous shell has formed on the surface of the up-conversion nanoparticles. The mesoporous structure of silica is derived from the condensation reaction of C18TMS and TEOS, in which the amount of C18TMS plays a key role in the formation of mesoporous structures with pore size distribution in the range of 2–10 nm owing to the use of C18TMS as a porogen.[31,32] Herein, our motivations are to achieve mesoporous silica-coated up-converted nanoparticles with higher specific surfaces, with a view for applications in the PDT of cancer cells. According to previous studies, the as-prepared samples with higher specific surfaces can be obtained when the optimal volume ratio of

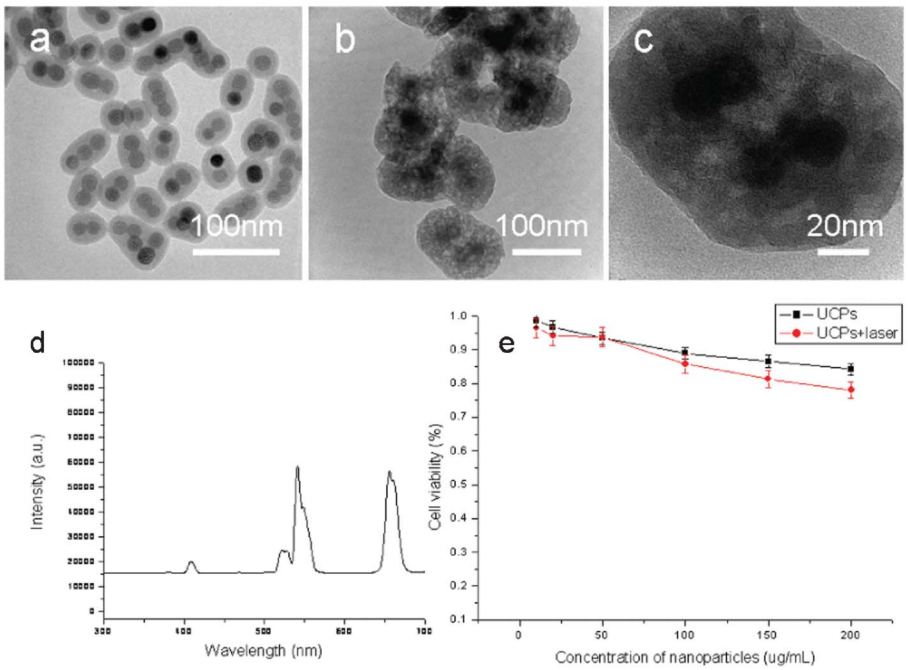

Fig. 3 TEM images of silica-coated nanocrystals obtained from 200 μL TEOS, 80 μL octadecyltrimethoxysilane (C18TMS) and 40 mL 0.04 M cyclohexane solution of $NaYF_4$ nanocrystals before calcination (a) and after calcination at 500 °C for 2 h (b–c); (d) fluorescence spectra of the $NaYF_4$:Yb/Er@mesoporous silica nanoparticles obtained from the samples shown in Fig. 3a after calcination at 500 °C for 2 h under excitation of 980 nm; (e) viability of cells incubated with the $NaYF_4$:Yb/Er@mesoporous silica nanoparticles.

TEOS and C18TMS is 5 : 2.[26,27] In the present study, a modified microemulsion process has been successfully developed to achieve water-soluble $NaYF_4$:Yb/Er@ mesoporous silica nanoparticles in which the specific surface area is higher than our previous protocol adopted to synthesize mesoporous silica-coated on $NaYF_4$:Yb/Er@silica nanoparticles.[26]

In vitro cytotoxicity tests and imaging

The viability of cells incubated with the $NaYF_4$:Yb/Er@mesoporous silica nanoparticles detected by MTS solution has been shown in Fig. 3e, in which there is no significant difference between cells treated with different concentrations. This suggested that the as-prepared particles are safe for biological applications even when the concentration of the particles reaches upto 200 μg mL^{-1}. Fig. 5 demonstrated the cell labeling with $NaYF_4$:Yb/Er@mesoporous silica nanoparticles. In Fig. 5, it can be seen that the live cells were successfully labeled and the specific fluorescence can be observed by NIR excitation using a confocal microscope equipped with a 980 nm NIR laser. The nanoparticles were mainly located at the cytoplasmic regions, which indicated that the as-synthesized composite nanoparticles are a potential candidate for the effective delivery of drugs and imaging labels.

Photodynamic therapy of cancer cells

UCNPs can be excited in the near-infrared (NIR) region and emit in the visible or NIR regions. This unique property makes them attractive for biological imaging because the NIR light

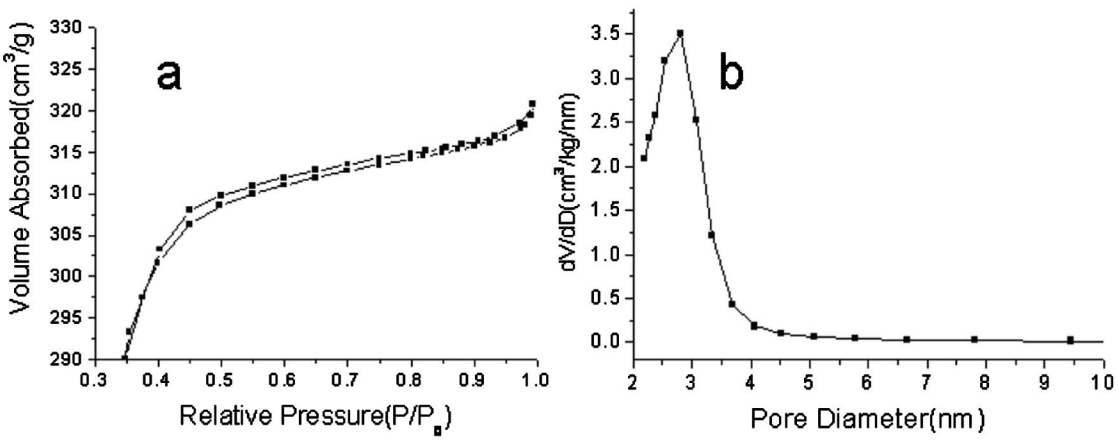

Fig. 4 N_2 adsorption–desorption isotherm (a), and pore-size distribution of mesoporous silica-coated $NaYF_4$:Yb/Er@silica nanoparticles (b).

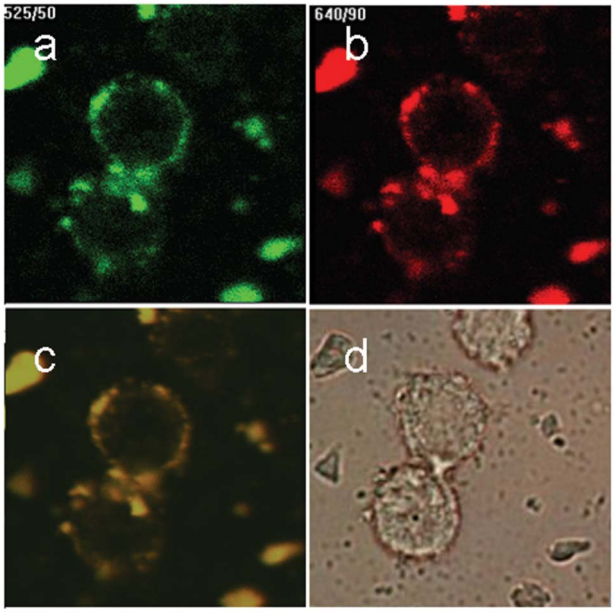

Fig. 5 (a–c) Total up-conversion fluorescence (yellow), and images upon passing through red or green filters of murine bladder cancer cells (MB49) after the uptake of mesoporous silica-coated $NaYF_4$:Yb/Er nanoparticles; the bright-field image is given in (d).

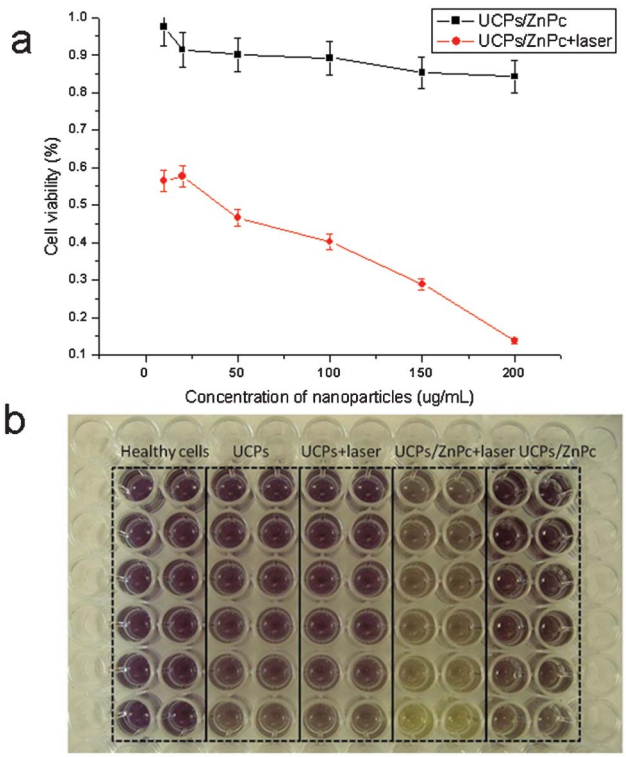

Fig. 6 Viability of cells incubated with the ZnPc-loaded nanoparticles as a function of the nanoparticle concentration, treated with or without NIR radiation. The incubated cells were exposed to NIR radiation for 5 min.

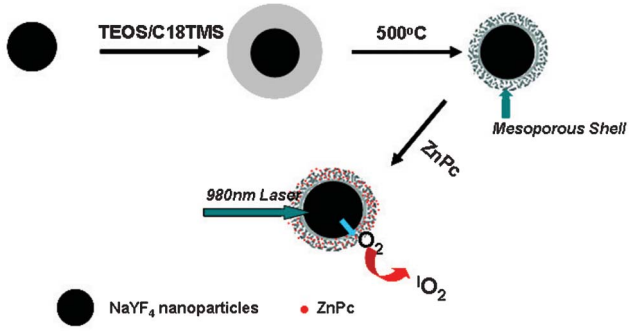

Fig. 7 Schematic illustration of the facile synthesis of a mesoporous silica-coating on the up-converted nanoparticles for the PDT of cancer cells with a 980 nm laser.

could better penetrate the tissue with minimal absorption/scattering. Subsequently, UCNPs have been widely used as a potential tool for in-depth imaging and PDT of deep tumor cells.[33] Fig. 6 shows the viability of cells incubated with ZnPc-loaded nanoparticles that were treated with and without NIR radiation for 5 min. The protocol for loading the ZnPc photosensitizer into the mesoporous layers of the core–shell up-converted nanoparticles can be found in our previous study.[26] As shown in Fig. 6a and b, upon excitation by a NIR laser for 5 min, the nanocrystals converted NIR radiation to visible light, which further activates the photosensitizer as the absorption peak of ZnPc at approximately 670 nm overlaps with the red emission peak of the up-converted $NaYF_4$ nanocrystals to release reactive singlet oxygen and kill cancer cells. The facile synthesis of mesoporous silica-coated UCNPs for PDT of cancer cells has been summarized in Fig. 7.

Conclusions

In summary, we have successfully synthesized mesoporous silica-coated $NaYF_4$:Yb/Er nanoparticles by a facile process. The nanoparticles displayed good biocompatibility and could be used for cell labeling. Furthermore, the $NaYF_4$:Yb/Er@silica composite nanoparticles incorporated with photosensitizers (ZnPc) exhibited a better performance for the photodynamic therapy of cancer cells by using UCNPs as remote controlled nano-transducers. Therefore, the as-synthesized core–shell nanoparticles will be of great importance in the potential applications of drug delivery and nanobiotechnology.[34]

Experimental

Reagents

YCl_3 (99%), $YbCl_3$ (99%), $ErCl_3$ (99%), IGEPAL CO-520, oleic acid and 1-octadecene were purchased from Sigma Chemic Ltd. Ammonia fluoride, sodium hydroxide, acetone, methanol, cyclohexane and ammonia solution (30 wt%) were purchased from Shanghai Chemical Ltd. All chemicals are of chemical grade and were used without further purification.

Preparation of uniform $NaYF_4$:Yb/Er nanocrystals

The synthesis process for the high quality hexagonal phase $NaYF_4$:Yb/Er nanocrystals can be found elsewhere.[23–24] In a

modified process, 0.80 mmol of YCl_3, 0.20 mmol of $YbCl_3$ and 0.02 mmol of $ErCl_3$ were added into a 100 ml three-neck round-bottom flask and dissolved using 2 mL of DI water to form a clear solution after vigorous stirring. Then, 6 mL of oleic acid and 15 mL of 1-octadecene were added into the previous solution which was heated up to 150 °C to form an oleic compound. Subsequently, the solution was cooled to room temperature naturally. Then, 4 mmol of NH_4F (0.1482 g) and 2.5 mmol of NaOH (0.1 g) in 10 mL of methanol was added, and then the solution was kept at 60 °C for 20 min. The solution was then heated to 300 °C under an argon atmosphere for 1 h and then cooled to room temperature naturally. The nanocrystals were precipitated with 10 mL of acetone and collected by centrifugation, and then redispersed in 100 mL of cyclohexane.

Preparation of mesoporous silica-coated $NaYF_4$:Yb/Er nanoparticles.

In a typical procedure, Igepal CO-520 (1.0 mL), cyclohexane (60 mL) and $NaYF_4$ nanocrystal solution in cyclohexane (40 ml, 0.04 M) were added into a 250 mL three-neck round-bottom flask and stirred for 10 min, respectively. Then, 0.8 mL ammonia (25–28 wt %) was added into the previous solution and sonicated for 20 min until a transparent emulsion was formed. The mixture solution of 200 μL TEOS and 80 μL octadecyltrimethoxysilane (C18TMS) was then added into the previous solution. Finally, the solution was stirred for 2 d at a speed of 600 rpm at room temperature. Silica-coated $NaYF_4$ nanoparticles were collected by centrifugation after precipitation by adding acetone, washed with ethanol three times and finally dried at 60 °C for 4 h. The as-prepared sample was calcinated at 500 °C in static air with a heating rate of 1 °C min^{-1} and a dwelling time of 2 h.

Cell labeling and imaging

MB49-PSA cells were seeded into 6-well plates. After being cultured for 24 h, the cells were immediately treated with nanoparticles at 100 μg mL^{-1}. Cells loaded with nanoparticles were fixed in 4% paraformaldehyde for 10 min at room temperature and then washed twice with 1× PBS for 5 min. The nuclei were counter-stained with 0.1 g ml^{-1} DAPI (Sigma) for 5 min at room temperature and then washed twice with 1× PBS for 5 min. Nanoparticles loaded into the fixed cells were then visualized under a confocal laser scanning microscope (Nikon C1 Confocal) specially fitted with a continuous wave 980 nm laser excitation source.

In vitro cytotoxicity tests

MB49-PSA cells were collected and diluted to a cell density of 1×10^5 mL^{-1} in complete medium, and then seeded into 96-well plates (100 μL $well^{-1}$). After being cultured for 24 h, the as-prepared samples with different concentrations (25, 50, 100, 200, 500 and 1000 μg mL^{-1}) were added to the cells and the cells were then incubated for 24 or 48 h at 37 °C. The cells were washed to remove the unbound nanoparticles. The cell viability was measured using the Cell Titer 96 Aqueous One Solution assay (Promega, Madison, WI) and was expressed as a percentage of the control.

Photodynamic effect of the nanoparticles on cancer cells

The protocol for the photodynamic effect of the nanoparticles can be found elsewhere.[7] First, the photosensitizer, zinc phthalocyanine (ZnPc), was loaded into the pores of the mesoporous silica by soaking the mesoporous silica-coated $NaYF_4$ nanoparticles (100 mg) in a 10 mL solution of ZnPc in pyridine (0.5 mg mL^{-1}) for 24 h at room temperature and collected by centrifugation. The MB49 cells were maintained at 37 °C in a humidified 5% CO_2 atmosphere and the nanoparticles (100 mg mL^{-1}) with and without ZnPc were added and incubated for 24 h and then exposed to a 980 nm laser with an output power of 500 mW for 5 min. The cells were then incubated at 37 °C for 1 d.

Characterization

The phase of the as-prepared product was characterized by XRD analysis, which was carried out on a Philips X'Pert PRO SUPER X-ray diffractometer equipped with graphite monochromatized Cu-Kα radiation and with the operation voltage and current maintained at 40 kV and 40 mA, respectively. The morphology and size of the samples were investigated by field-emission scanning electron microscopy (FESEM, JEOL-6700F) and TEM (JEOL 3010). The BET specific surface area and pore size distributions of the sample were carried out on Quantachrome Autosorb-1 (Quantachrome, USA). Before measurement, the samples were degassed in a vacuum at 200 °C for more than 3 h. The method was utilized to calculate the specific surface areas. BET, the pore volumes and the pore size distributions were derived from the desorption branches of the isotherms by the Barrett–Joyner–Halenda (BJH) model, and the total pore volumes were estimated from the adsorbed amount at a relative pressure (P/P_0) of 0.992. The fluorescence images were captured in bright field and under infrared excitation using a Nikon confocal microscope. Fluorescence spectra were recorded on a SpectroPro 2150i spectrophotometer equipped with a 1200 g mm^{-1} grating and a 980 nm VA-II diode pumped solid-state (DPSS) laser.

Acknowledgements

H.S.Q acknowledges the financial support by the National Science Foundation of China (Grants No. 21101140, 31100688, 51102215), the Zhejiang Provincial Natural Science Foundation of China (Grants No.Y4110025), the Zhejiang Qianjiang Talent Project (2012R10062), and the Foundation of Science and Technology Committee of Gansu (1102NKDA033). The authors additionally acknowledge the International Science and Technology Cooperation Program of Gansu (1104WCGA185), the Scientific Research Foundation for the Returned Overseas Chinese Scholars, the State Education Ministry, and the Doctoral Start-up Foundation of Zhejiang Normal University.

References

1 L. Zhou, Y. W. Ning, S. H. Wei, Y. Y. Feng, J. H. Zhou, B. Y. Yu and J. Shen, *J. Mater. Sci.: Mater. Med.*, 2010, **21**, 2095–2101.
2 R. Lin, L. Zhou, K. L. Fang, Y. Lin, A. Wang, J. H. Zhou, S. H. Wei and J. Mater, *J. Mater. Sci.: Mater. Med.*, 2012, **23**, 1629–1635.
3 J. Klesing, A. Wiehe, B. Gitter, S. Graefe and M. Epple, *J. Mater. Sci.: Mater. Med.*, 2010, **21**, 887–892.
4 G. S. Yi, H. C. Lu, S. Y. Zhao, G. Yue, W. J. Yang, D. P. Chen and L. H. Guo, *Nano Lett.*, 2004, **4**, 2191–2196.
5 C. X. Li and J. Lin, *J. Mater. Chem.*, 2010, **20**, 6831–6847.
6 J. Zhou, Z. Liu and F. Y. Li, *Chem. Soc. Rev.*, 2012, **41**, 1323–1349.

7 H. C. Guo, H. S. Qian, N. M. Idris and Y. Zhang, *Nanomed.: Nanotechnol., Biol. Med.*, 2010, **6**, 486–495.
8 S. L. Gai, P. P. Yang, C. X. Li, W. X. Wang, Y. L. Dai, N. Niu and J. Lin, *Adv. Funct. Mater.*, 2010, **20**, 1166–1172.
9 L. Y. Wang, R. X. Yan, Z. Y. Huo, L. Wang, J. H. Zeng, J. Bao, X. Wang, Q. Peng and Y. D. Li, *Angew. Chem., Int. Ed.*, 2005, **44**, 6054–6057.
10 L. Xiong, Z. Chen, M. Yu, F. Li, C. Liu and C. H. Huang, *Biomaterials*, 2009, **30**, 5592–5600.
11 A. Aebischer, M. Hostettler, J. Hauser, K. Krämer, T. Weber, H. U. Güdel and H. B. Buergi, *Angew. Chem., Int. Ed.*, 2006, **45**, 2802–2806.
12 H. X. Mai, Y. W. Zhang, R. Si, Z. G. Yan, L. D. Sun, L. P. You and C. H. Yan, *J. Am. Chem. Soc.*, 2006, **128**, 6426–6436.
13 J. C. Boyer, L. A. Cuccia and J. A. Capobianco, *Nano Lett.*, 2007, **7**, 847–852.
14 C. X. Li, Z. W. Quan, J. Yang, P. P. Yang and J. Lin, *Inorg. Chem.*, 2007, **46**, 6329–6337.
15 X. Liang, X. Wang, J. Zhuang, Q. Peng and Y. D. Li, *Inorg. Chem.*, 2007, **46**, 6050–6055.
16 L. Y. Wang and Y. D. Li, *Nano Lett.*, 2006, **6**, 1645–1649.
17 L. Y. Wang and Y. D. Li, *Chem. Mater.*, 2007, **19**, 727–734.
18 F. Wang, Y. Han and X. G. Liu, *Nature*, 2010, **463**, 106l–1065.
19 Z. G. Chen, H. L. Chen, M. X. Yu, F. Y. Li, Q. Zhang, Z. G. Zhou, T. Yi and C. H. Huang, *J. Am. Chem. Soc.*, 2008, **130**, 3023–3029.
20 Z. Q. Li, S. Jiang and Y. Zhang, *Adv. Mater.*, 2008, **20**, 4765–4769.
21 S. Nagarajan and Y. Zhang, *Nanotechnology*, 2011, **22**, 395101.
22 L. Y. Ang, M. E. Lim, L. C. Ong and Y. Zhang, *Nanomedicine*, 2011, **6**, 1273–1288.
23 Z. Q. Li and Y. Zhang, *Nanotechnology*, 2008, **19**, 345606.
24 H. S. Qian and Y. Zhang, *Langmuir*, 2008, **24**, 12123–12125.
25 R. Hild, C. David, H. U. Müller, B. Völkel, D. R. Kayser and M. Grunze, *Langmuir*, 1998, **14**, 342–346.
26 H. S. Qian, H. C. Guo, P. C. L. Ho, R. Mahendran and Y. Zhang, *Small*, 2009, **5**, 2285–2290.
27 D. K. Yi, S. S. Lee, G. C. Papaefthymiou and J. Y. Ying, *Chem. Mater.*, 2006, **18**, 614–619.
28 M. Kim, K. Sohn, B. H. Na and T. Hyeon, *Nano Lett.*, 2002, **2**, 1383–1387.
29 J. F. Suyver, A. Aebischer, D. Biner, P. Gerner, J. Grimm, S. Heer, K. W. Krämer, C. Reinhard and H.U. Güdel, *Opt. Mater.*, 2005, **27**, 1111–1130.
30 K. S. W. Sing, *Pure Appl. Chem.*, 1957, **87**, 603.
31 Y. Y. Yin, M. Chen, S. X. Zhou and L. M. Wu, *J. Mater. Chem.*, 2012, **22**, 11245.
32 Y. Chen, H. R. Chen, L. M. Guo, Q. J. He, F. Chen, J. Zhou, J. W. Feng and J. L. Shi, *ACS Nano*, 2010, **4**, 11245.
33 D. K. Chatterjee and Y. Zhang, *Nanomedicine*, 2008, **3**, 73–82.
34 D. K. Chatterjee, M. K. Jayakumar and Y. Zhang, *Small*, 2010, **6**, 2781–2795.